JACS
JOURNAL OF THE AMERICAN CHEMICAL SOCIETY
Article
pubs.acs.org/JACS

Tailoring Porphyrin-Based Electron Accepting Materials for Organic Photovoltaics

Jeff Rawson,[†] Andrew C. Stuart,[‡] Wei You,*[,‡] and Michael J. Therien*[,†]

[†]Department of Chemistry, French Family Science Center, Duke University, 124 Science Drive, Durham, North Carolina 27708-0346, United States

[‡]Department of Chemistry, University of North Carolina at Chapel Hill, Chapel Hill, North Carolina 27599-3290, United States

Supporting Information

ABSTRACT: The syntheses, potentiometric responses, optical spectra, electronic structural properties, and integration into photovoltaic devices are described for ethyne-bridged isoindigo-(porphinato)zinc(II)-isoindigo chromophores built upon either electron-rich 10,20-diaryl porphyrin (Ar-Iso) or electron-deficient 10,20-bis(perfluoroalkyl)porphyrin (Rf-Iso) frameworks. These supermolecules evince electrochemical responses that trace their geneses to their respective porphyrinic and isoindigoid subunits. The ethyne linkage motif effectively mixes the comparatively weak isoindigo-derived visible excitations with porphyrinic $\pi-\pi^*$ states, endowing Ar-Iso and Rf-Iso with high extinction coefficient ($\varepsilon \sim 10^5$ $M^{-1}\cdot cm^{-1}$) long-axis polarized absorptions. Ar-Iso and Rf-Iso exhibit total absorptivities per unit mass that greatly exceed that for poly(3-hexyl)thiophene (P3HT) over the 375−900 nm wavelength range where solar flux is maximal. Time-dependent density functional theory calculations highlight the delocalized nature of the low energy singlet excited states of these chromophores, demonstrating how coupled oscillator photophysics can yield organic photovoltaic device (OPV) materials having absorptive properties that supersede those of conventional semiconducting polymers. Prototype OPVs crafted from the poly(3-hexyl)thiophene (P3HT) donor polymer and these new materials (i) confirm that solar power conversion depends critically upon the driving force for photoinduced hole transfer (HT) from these low-band-gap acceptors, and (ii) underscore the importance of the excited-state reduction potential ($E^{-/*}$) parameter as a general design criterion for low-band-gap OPV acceptors. OPVs constructed from Rf-Iso and P3HT define rare examples whereby the acceptor material extends the device operating spectral range into the NIR, and demonstrate for the first time that high oscillator strength porphyrinic chromophores, conventionally utilized as electron donors in OPVs, can also be exploited as electron acceptors.

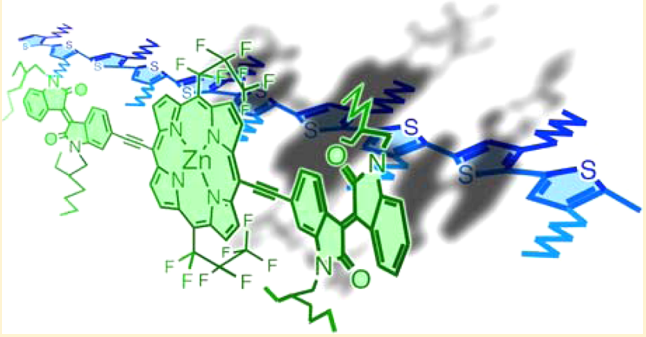

INTRODUCTION

A principal challenge in the design of next generation organic photovoltaics (OPVs) lies in engineering materials that provide high absorptivity (extinction coefficient $\varepsilon > 10^4$ $M^{-1}\cdot cm^{-1}$) over the spectral range corresponding to the solar irradiance spectrum at the earth's surface. The Air Mass 1.5 (AM1.5) solar irradiance spectrum provides a measure of the sun's energy to reach earth's surface in units of $W\cdot m^{-2}\cdot nm^{-1}$; it is most intense (>0.75 $W\cdot m^{-2}\cdot nm^{-1}$) between 375 and 900 nm, and 66% of the total flux lies within this range.[1] Because of the inverse proportionality between film thickness and charge collection efficiency, there is a motivation to craft OPV films that are thinner than 100 nm, yet capable of capturing most of the incident 375−900 nm light.[2] Optimizing the absorptive oscillator strength of electron donor (D) and acceptor (A) materials over the 375−900 nm spectral domain is thus critical to next-generation OPV design.

Poly(3-hexylthiophene) (P3HT) and phenyl-C_{61}-butyric acid methyl ester (PCBM) are the best studied OPV materials and continue to stand as benchmarks in this field.[3] The development of new polymers with lower optical band gaps and larger per mass absorptivities than those of P3HT has advanced rapidly,[4] and devices that blend these polymers with fullerene electron acceptors have achieved power conversion efficiencies (η) as high as 9.2% for single junction[4d] and 10.6% for tandem devices.[5] Great strides have been made using monodisperse alternatives to polymeric materials,[6] culminating in the recent disclosure of an 8.9% efficient solar cell that employed a silolodithiophene-derived donor and phenyl-C_{71}-butyric acid methyl ester acceptor.[6h]

Considerably less progress has been made toward designing new organic acceptor materials that might replace fullerenes, and summaries of the state of the art in OPV development sometimes ignore this category altogether.[7] The immaturity of efforts in this area contrasts the potential impact of molecular

Received: September 21, 2014
Published: November 20, 2014

   dx.doi.org/10.1021/ja5097418 | J. Am. Chem. Soc. 2014, 136, 17561−17569

electron acceptors that absorb broadly over the vis-NIR spectral domain at high oscillator strength, as fullerenes such as PCBM are characterized by faint visible-range electronic transitions that are known to contribute negligibly to photocurrent.[2c] Electron-deficient pigments such as perylene diimide,[8] boron perfluorosubphthalocyanine,[9] isoindigo, or perfluoralkylporphyrins[10] are characterized by $S_0 \rightarrow S_1$ transitions in the range of 500−600 nm with ε on the order of 10^4 L·mol^{-1}·cm^{-1}. When these easily reduced pigments are coupled to electron-rich moieties such as thiophene derivatives[11] or amine groups,[12] push−pull chromophores result that can have NIR intramolecular charge transfer (ICT) absorption bands with onsets as low as 800 nm and maxima as large as ∼5 × 10^4 L·mol^{-1}·cm^{-1}. The spectral characteristics of these push−pull chromophores are impressive; however, when they are employed as acceptor materials in OPVs, it is often found that a negligible portion of the devices' photocurrent can be attributed to acceptor excitation.[11b]

A potent alternative method for crafting high oscillator strength, broad spectral domain absorbers involves coupling multiple pigment motifs via ethyne bridges in a manner that aligns their component transition dipoles.[13,14] Such coupled-oscillator architectures, composed of building-block pigments capable of significant charge-resonance interactions, provide supermolecular chromophores that exhibit large polarizabilities and hyperpolarizabilities, and electronically excited states that manifest extensive spatial delocalization. With respect to designing a supermolecular electron acceptor (A) for OPV applications, additional considerations include: (i) an acceptor LUMO level (an $A^{-/0}$ potential) appropriate for electron transfer (ET) from the photoexcited donor (^{1}D*), (ii) a corresponding electronic excited state (^{1}A*) having sufficient thermodynamic driving force (an $A^{-/*}$ potential) to facilitate ^{1}A*-to-D hole transfer (HT), and (iii) high oscillator strength absorptivity across a broad range of vis-NIR wavelengths.

Porphyrin derivatives are well-known for their strong coloration, and the prevalence of this motif in biological light-harvesting structures has inspired incorporation of this conjugated unit into a wealth of functional materials.[15] One strategy for augmenting the distribution, breadth, and intensities of the porphyrin-derived absorption bands is to extend the conjugated framework by attaching various aromatic groups using ethyne bridges at the macrocycle *meso* positions.[13,14,16,17] Some such ethyne-extended porphyrins have been employed as donor materials in OPVs[18] as well as dye sensitized solar cells.[19] The porphyrin motif has been heretofore unrepresented as an OPV molecular acceptor due to its inherently electron-rich nature; congruent with this fact, the few reported attempts to achieve charge separation in porphyrin/P3HT blends did not meet with success (for example, such exemplary OPVs showed power conversion efficiencies < 0.01%).[20] Electron-deficient *meso*-(perfluoroalkyl)porphyrins, characterized by energy levels suitable for application to the molecular acceptor problem, have been devised;[10,21] while such structures have been incorporated into supermolecular chromophores,[13f] they have yet to be conjugated to complementary electron-poor pigment motifs.

N,*N*′-Dialkyl isoindigo and related structures define an emergent class of technologically important electron-deficient chromophores;[22] for example, isoindigo has served as a building block for n-type and ambipolar polymers that possess electron mobilities as high as 0.6 cm^2·V^{-1}·s^{-1}.[23] While this structural motif has become quite common in donor polymers[24] and small molecules[11c,25] for OPVs, there is only one report of isoindigo polymers being used as OPV acceptor materials.[26] Isoindigo, while a classic dye motif, possesses modest vis-spectral domain oscillator strength;[27] incorporation of the isoindigo motif into electron accepting materials for OPVs is further discouraged by the rapid depopulation of its excited state due to fast nonradiative decay.[27]

We report herein supermolecular chromophores based on ethyne-linked (porphinato)zinc (PZn) and isoindigo (Iso) units that exhibit intense panchromatic absorptions, long-lived S_1 states, and LUMO energy levels suitably poised for photoinduced electron transfer from P3HT. Because these materials feature higher absorptivities per unit mass than P3HT in the critical 375−900 nm window, they have the potential to contribute significantly to light harvesting in OPVs. The availability of both electron rich *meso*-diarylporphyrin and electron deficient *meso*-bis(perfluoroalkyl)porphyrin building blocks allows the syntheses of two archetypal PZn-Iso chromophores, [5,15-bis(*N*,*N*′-bis(2-ethylhexyl)-6-isoindigoyl)-ethynyl-10,20-bis(2,6-(3,3-dimethyl-1-butyloxy)phenyl)-porphinato]zinc(II) (Ar-Iso) and [5,15-bis(*N*,*N*′-bis(2-ethylhexyl)-6-isoindigoyl)ethynyl-10,20-bis(heptafluoropropyl)-porphinato]zinc(II) (Rf-Iso). The isoindigo moiety in these chromophores determines the $A^{-/0}$ potential; because the [5,15-bis(perfluoroalkyl)porphinato]zinc(II) unit possesses a HOMO level ∼0.3 eV stabilized with respect to that of [5,15-diphenylporphinato]zinc(II),[10b,13f] Ar-Iso and Rf-Iso permit direct evaluation of the significance of the chromophore excited state reduction potential ($A^{-/*}$) as a design parameter in OPVs where the acceptor's absorptive properties strongly contribute to the photocurrent. This study illustrates how manipulation of coupled oscillator photophysics can yield conjugated acceptor materials that feature visible-light absorptivities that supersede those of conventional semiconducting polymers and electronically excited states that possess large driving forces for photoinduced hole transfer; furthermore, this work demonstrates for the first time that high oscillator strength porphyrinic chromophores, conventionally used as electron donors, can also be exploited as electron acceptors in OPVs.

■ EXPERIMENTAL SECTION

Ar-Iso and Rf-Iso syntheses were accomplished via palladium-catalyzed cross coupling reactions involving, respectively, (5,15-diethynyl-10,20-bis(2′,6′-bis(3,3-dimethyl-1-butoxy)phenyl)porphinato)zinc(II)[14a] and (5,15-diethynyl-10,20-bis(heptafluoropropyl)porphinato)zinc(II) with 6-Br-*N*,*N*′-bis(2-ethylhexyl)isoindigo.[13f] Further details regarding the syntheses, purification, and characterization of Ar-Iso and Rf-Iso can be found in the Supporting Information.

Cyclic voltammetric experiments carried out in solution were performed in tetrahydrofuran (THF) solvent containing 0.1 M Bu_4NPF_6 as supporting electrolyte. For measurements in the solid state, films were drop-casted onto a platinum electrode from THF solutions and dried under vacuum; the cyclic voltammetric responses of these thin films were acquired in acetonitrile solvent containing 0.1 M Bu_4NPF_6. All electrochemical measurements utilized scan rates that ranged between 100 and 200 mV·s^{-1}, and ferrocene as an internal potentiometric standard.

Bilayer photovoltaic devices were made from 15 mg·mL^{-1} solutions of P3HT in *o*-dichlorobenzene (DCB) and 10 mg·mL^{-1} solutions of Rf-Iso or Ar-Iso in 4:1 DCB:THF. The P3HT layer was spin-cast first between 400−800 rpm for 30−60 s onto the poly(3,4-ethylenedioxythiophene)/polystyrenesulfonate (PEDOT:PSS) layer, following which the solvent was evaporated at room temperature under N_2 for 12 h. The acceptor was then spin-cast from 4:1 DCB:THF onto

dx.doi.org/10.1021/ja5097418 | J. Am. Chem. Soc. 2014, 136, 17561−17569

the P3HT films between 400 and 800 rpm for 30−60 s, and dried as noted for the initial P3HT film. The cathodes were deposited by thermal evaporation of 100 nm of aluminum with a shadow mask at a pressure of ∼1 × 10^{-6} mbar. Device characterization was carried out under AM 1.5G irradiation and a light intensity of 100 mW·cm^{-2} (Oriel 91160, 300 W), which was calibrated using a NREL-certified standard silicon cell. All fabrication steps after adding the PEDOT:PSS layer onto ITO substrate, and all *I*−*V* characterization, were performed in a glovebox under nitrogen atmosphere. Further details are provided in the Supporting Information.

All electronic structure calculations were performed upon model compounds in which aliphatic chains were truncated to methyl groups (Supporting Information). Structure optimization and linear response calculations were performed with density functional theory (DFT) using Gaussian 09, revision C.1.[28] The Becke three-parameter hybrid[29] and the Lee−Yang−Parr correlation functional[30] were employed for all calculations (B3LYP). Optimizations were performed with minimal symmetry constraints using tight optimization criteria; initial optimizations used smaller basis sets but the final optimizations and TDDFT calculations employed the 6-311+g basis set[31] as implemented in Gaussian 09.

Selected frontier orbital wave functions were plotted as isosurfaces (iso = 0.02) using Gaussview 5.[32] This software was also used to produce S_1 state electron density difference plots for Ar-Iso and Rf-Iso by subtracting the ground state density from the excited state electron density distribution; this electron density difference was displayed as a mapped isosurface onto the ground state density (isosurface value = 0.002). TDDFT result files were postprocessed using the GaussSum package;[33] this software partitions the wave function amplitudes onto atomic components using Mulliken population analysis,[34] and parses the electronic configurations contributing to each excitation. Transition dipole moment vectors were plotted using VMD.[35]

RESULTS AND DISCUSSION

Supermolecular Chromophores Ar-Iso and Rf-Iso. The molecular structures of Ar-Iso and Rf-Iso are shown in Chart 1. Figure 1 displays the electronic absorption spectra acquired over the 375−850 nm spectral domain for supermolecular acceptors Ar-Iso and Rf-Iso, and the classic OPV benchmark materials, P3HT and PCBM. Electronic absorption spectra recorded for the Ar-Iso and Rf-Iso chromophoric building blocks are displayed in the Supporting Information. To facilitate quantitative absorptivity comparisons between these molecular and benchmark polymeric materials, Figure 1 spectra are reported in units of (absorbance·L)/(g·cm); this expresses the intrinsic light harvesting capacity of these materials on a basis of direct relevance to device applications, where compositions are typically reported as weight ratios.[36] To permit comparisons of the total visible range absorptivity per unit mass, integrations of these spectra from 375 to 850 nm are depicted in the upper panel of Figure 1. Note that Ar-Iso and Rf-Iso provide high intrinsic absorptivity over the 375−850 nm window relative to classic OPV donor and acceptor chromophores: as evident in Figure 1 data, Ar-Iso and Rf-Iso feature mass-normalized absorbances approximately twice that of P3HT, and over 23 times that manifested by PCBM (Figure 1).

Chart 1. Structures of Chromophores Rf-Iso and Ar-Iso, Key Precursor Molecules, and Benchmark OPV Materials

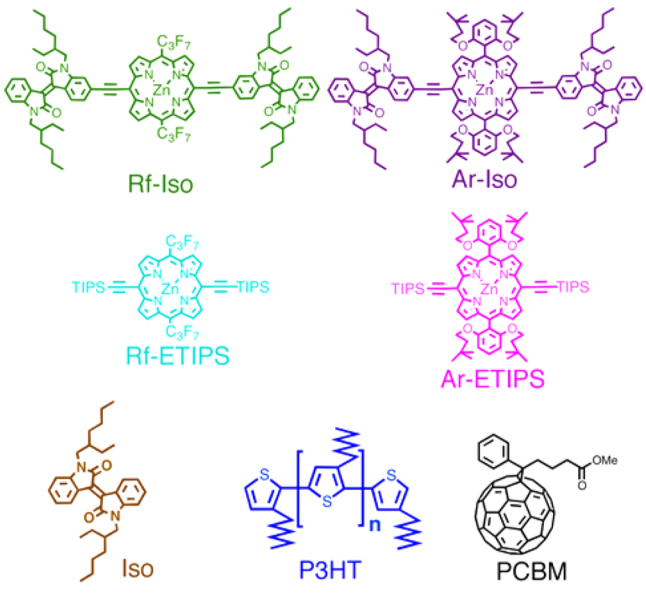

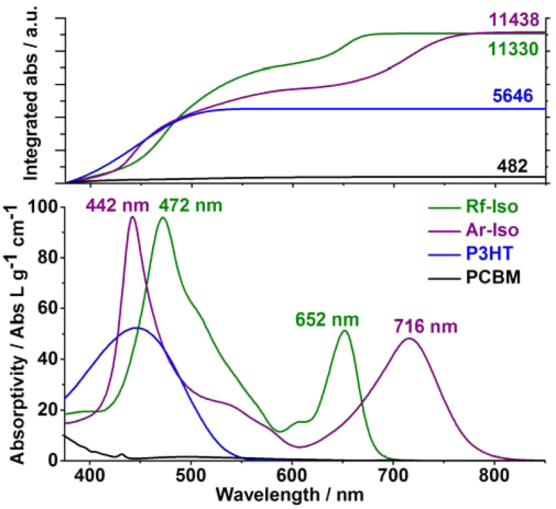

Figure 1. (Bottom) Electronic absorption spectra of Rf-Iso, Ar-Iso, P3HT, and PCBM in THF solvent normalized by mass. (Top) Integrated, mass-normalized absorption spectra of these chromophores determined over the 375−850 nm spectral range.

Rf-Iso and Ar-Iso evince Q-state derived transitions centered at 652 and 716 nm, respectively; note that the extinction coefficients for these absorptive maxima exceed 10^5 M^{-1}·cm^{-1} (Table 1). The high oscillator strengths of these absorptions (f > 0.3; Table 1) derive from frontier orbital degeneracies for these supermolecules which are greatly diminished (Figure S1) compared with their respective parent (porphinato)zinc (PZn) building blocks, Ar-ETIPS and Rf-ETIPS (Figure S2), leading to modest degrees of configuration interaction for their lowest energy electronic transitions. Time-dependent DFT calculations confirm the long-axis polarizations of these supermolecular Q-state derived transitions. This reduction in configuration interaction relative to that evident for the parent PZn framework is particularly dramatic for Rf-Iso: note all major vis-spectral domain transitions for this chromophore lie parallel to its long axis, whereas for Rf-ETIPS *x*- and *y*-polarized excitations contribute approximately equally to the transitions that lie in this spectral region (Figure S3). Commensurate with this reorientation of the principal optical axis in Rf-Iso, a dramatic increase of Q-domain absorptive oscillator strength relative to the Rf-ETIPS benchmark is also evident (Table 1). In these Rf-Iso and Ar-Iso supermolecules, the Iso units direct significant redistributions of PZn-derived oscillator strength due to the head-to-tail alignment of the PZn and Iso low energy transition dipoles and the substantial interactions between the

dx.doi.org/10.1021/ja5097418 | J. Am. Chem. Soc. 2014, 136, 17561−17569

Table 1. Absorption Band Maxima, Energies, Extinction Coefficients, Full Widths at Half Maximum (FWHM), and Oscillator Strengths of PZn-Isoindigo Compounds and Chromophoric Benchmarks in THF Solvent

	B-band region					Q-band region					total
compd	λ/nm	ν/cm^{-1}	log(ε)	fwhm/cm^{-1}	oscillator strength	λ/nm	ν/cm^{-1}	log(ε)	fwhm/cm^{-1}	oscillator strength	oscillator strength
Iso	368	27 174	4.10	–	0.105[b]	494	20 243	3.55	–	0.048[c]	0.153[a]
	391	25 575	4.08								
Ar-ETIPS	439	22 779	5.66	792	1.345[d]	540	18 519	3.52	367	0.126[e]	1.471[a]
						582	17 182	4.12			
						635	15 748	4.69			
Rf-ETIPS	444	22 523	5.70	547	1.256[d]	568	17 606	4.03	–	0.078[e]	1.334[a]
						590	16 949	4.16			
						635	15 748	3.31			
Ar-Iso	442	22 624	5.27	2143	1.994[f]	716	13 966	4.97	1547	0.514[g]	2.508[a]
Rf-Iso	472	21 186	5.22	3278	2.077[h]	652	15 337	4.95	903	0.318[i]	2.395[a]

[a]Oscillator strengths calculated over the 375−850 wavelength domain. [b]Oscillator strength calculated over the 375−445 wavelength domain. [c]Oscillator strength calculated over the 445−850 wavelength domain. [d]Oscillator strengths calculated over the 375−485 wavelength domain. [e]Oscillator strengths calculated over the 485−850 wavelength domain. [f]Oscillator strength calculated over the 375−608 wavelength domain. [g]Oscillator strength calculated over the 608−850 wavelength domain. [h]Oscillator strength calculated over the 375−587 wavelength domain. [i]Oscillator strength calculated over the 587−850 wavelength domain.

Iso and 5,15-diethynyl(porphinato)zinc fragment frontier orbitals (Figure S1).[13m,14,37]

The spatial distributions of the frontier orbital wave functions, and the first excited state electron density difference maps for the Rf-Iso and Ar-Iso supermolecules, reveal that Ar-Iso features significantly more charge-resonance character in its low-lying singlet excited state relative to Rf-Iso (Figure 2). In spite of the strong coupling provided by the ethyne bridges, the energetic mismatch between the PZn and Iso fragment energy levels restricts the extent of electronic delocalization within the frontier orbitals; note that Iso atom-derived electron density contributes only 20% to the Ar-Iso HOMO amplitude, but 78% to the corresponding Ar-Iso LUMO amplitude. Photoexcitation of Ar-Iso thus redistributes electron density from the PZn to the Iso unit, giving rise to a delocalized S_1 state having substantial charge-resonance character. Due to the σ-electron withdrawing character of the *meso*-perfluoroalkyl substituents, the HOMO and LUMO of the [5,15-bis(perfluoroalkyl)-porphinato]zinc(II) unit are equivalently stabilized by ∼0.3 eV relative to the corresponding orbitals of [5,15-diphenylporphinato]zinc(II);[10a,b,13f,21c] as a result, the Rf-Iso frontier orbitals feature similar wave function amplitude contributions from the PZn and Iso building blocks. Likewise, the first excited state electron density difference map for Rf-Iso resembles that of a classic, delocalized $\pi-\pi^*$ electronic transition. While the S_1 state electron density distributions differ for Rf-Iso and Ar-Iso, these chromophores possess significant and similar Q-state derived transition oscillator strengths (Table 1), congruent with large dispersions of their frontier orbital energy levels (Figure S1).[16c,38]

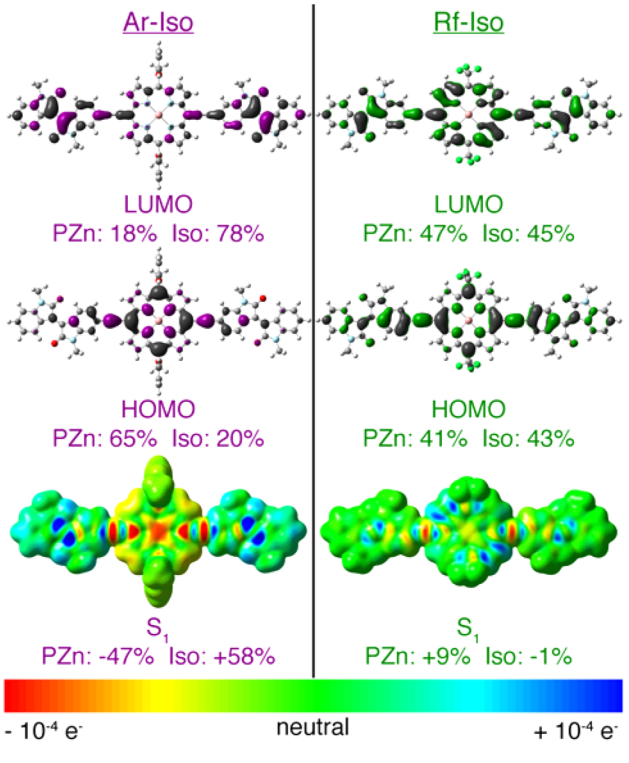

Figure 2. Frontier molecular orbitals and first excited state density differences for Ar-Iso and Rf-Iso plotted as 0.02 (orbitals) and 0.002 (densities) isodensity surfaces. Percentages reflect the ratio of orbital coefficients contributed from either the PZn or Iso fragments, excluding ethyne carbons, as determined by population analysis.

Figure S4 displays electronic absorption spectra of films of Ar-Iso and Rf-Iso drop-casted from THF solutions. The low-energy absorption band maxima observed for the Ar-Iso (739 nm) and Rf-Iso (685 nm) films lie, respectively, 1292 and 1732 cm^{-1} to the red of their corresponding Q-state-derived transitions in solution, consistent with significant π-cofacial intermolecular interactions in the solid state.[11c,39] The greater thin film transition red-shift observed for Rf-Iso is congruent with its sterically unencumbering *meso*-perfluoroalkyl substituents: the 2′,6′-disubstituted *meso*-aryl substituents of Ar-Iso partially shroud the porphyrin plane and attenuate the extent of intermolecular interactions in the thin film.[13n] Importantly, the solid-state absorption spectral onset (E_g) values for Ar-Iso and Rf-Iso are 1.571 and 1.687 eV, respectively, significantly below the ∼1.9 eV onset for P3HT.

The potentiometric data acquired for these compounds determined in THF solvent reveal responses that trace their genesis to the redox processes of their respective chromophoric subunits (Table 2; Figure S5). The cathodic electrochemical responses for Ar-Iso and Rf-Iso display two isoindigo-centered 1-electron reduction events. Cyclic voltammetric data show that for Ar-Iso, these Iso$^{-/0}$ and Iso$^{2-/-}$ redox processes occur at

dx.doi.org/10.1021/ja5097418 | J. Am. Chem. Soc. 2014, 136, 17561−17569

Table 2. Potentiometric Data Determined in THF Solvent or Thin Films Referenced to a Fc/Fc^+ Internal Standard

compd	$Iso^{-/0}$	$Iso^{-/2-}$	$PZn^{-/0}$	$PZn^{0/+}$
Iso	−1.389	−1.792	N/A	N/A
Ar-Etips	N/A	N/A	−1.830	−[b]
Rf-Etips	N/A	N/A	−1.361	−[c]
Ar-Iso (THF)	−1.248	−1.633	−2.078	0.353
Ar-Iso (film)	−1.234	−[d]	−[d]	0.300
Rf-Iso (THF)	−1.218	−1.711	−1.435	−[c]
Rf-Iso (film)	−1.204	−[d]	−[d]	0.757

[a]Experimental conditions: [chromophore] = 1−3 mM; scan rate = 200 mV s^{-1}; reference electrode = Ag/AgCl; solvent = THF/0.1 M NBu_4PF_6. [b]Not measured. [c]Oxidation lay outside the solvent's electrochemical window. [d]Only first reduction is reported.

higher potential than that for the (porphinato)zinc(II)-centered 1-electron reduction [$E_{1/2}(PZn^{-/0}) = -2.078$ V]; in contrast, for Rf-Iso, the potentials of these two Iso-centered reductions bracket $E_{1/2}(PZn^{-/0})$ [$(E_{1/2}(Iso^{-/0}) = -1.218$ V; $E_{1/2}(PZn^{-/0}) = -1.435$ V; $E_{1/2}(Iso^{2-/-}) = -1.711$ V; Figure S5]. These data evince the closer energetic matching of the low-lying empty Iso and PZn fragment molecular orbitals in Rf-Iso relative to Ar-Iso, congruent with electronic structure calculations. Cyclic voltammetric measurements carried out on thin film samples of these compositions found onset potentials of similar magnitude to the solution $E_{1/2}$ values determined for the initial oxidative and reductive processes of Rf-Iso and Ar-Iso (Table 2; Figure S6).

The energy of formation for free charges from excitons ($-\Delta G_{CS}$) quantifies the thermodynamic driving force for electron or hole transfer between a given D/A pair at organic semiconductor junctions; this can be evaluated using formalism developed by Weller.[40] The donor and acceptor excited state oxidation ($D^{*/+}$) and reduction ($A^{-/*}$) potentials can be estimated from $D^{0/+}$ and $A^{-/0}$ determined potentiometrically and E_g determined by absorption onset.[40c] The effective work function for the ferrocene/ferrocenium ($Fc^{0/+}$) couple of −4.8 eV relates the potentiometric data acquired for thin films of these materials to an absolute scale by $E_{vac} = -e(4.8 + E_{po})$,[41] where E_{vac} is the vacuum energy level and E_{po} are the electrochemically measured potentials. For values of E_g, $D^{0/+}$, and $A^{-/0}$ determined from measurements in the solid state, where excitonic effects can enhance the mismatch between optical and potentiometric band gaps, a correction factor $\Delta = (E^{-/0} - E^{0/+}) - E_g$ can be used to provide a more accurate estimate of the singlet exciton energy.[40c,d] The excited state reduction potential is then

$$E^{-/*} = E^{-/0} - \left(\frac{1}{2}\Delta + E_g\right) = E^{0/+} + \frac{1}{2}\Delta$$

and the excited state oxidation potential is

$$E^{*/+} = E^{0/+} + \left(\frac{1}{2}\Delta + E_g\right) = E^{-/0} - \frac{1}{2}\Delta$$

These values for Ar-Iso, Rf-Iso, and P3HT are displayed as dashed lines in Figure 3. The free energies of charge separation ΔG_{CS} between two materials X and Y are then

$$\Delta G_{CS} = X^{-/*} - Y^{0/+}$$

for hole transfer (HT) and

$$\Delta G_{CS} = X^{-/0} - Y^{*/+}$$

for electron transfer (ET), respectively.

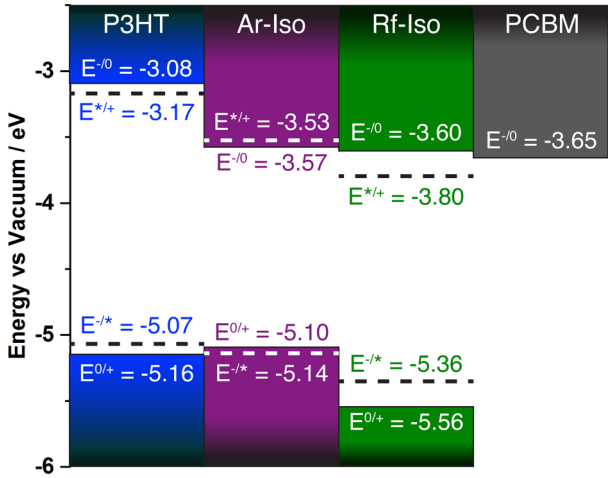

Figure 3. (Solid rectangles) Potentiometrically determined frontier energy levels for P3HT, Ar-Iso, and Rf-Iso in thin films compared with the PCBM reference; all energy levels are versus the vacuum energy and determined by the relation $E_{vac} = -e(4.8 + E_{ox/red})$. (Dashed lines) Excited state redox potentials for P3HT, Ar-Iso, and Rf-Iso determined by adding the singlet excitation energy E_g to the ground state frontier levels.

These considerations indicate that electronically excited P3HT (^{1}P3HT*) should undergo photoinduced ET reactions with both Ar-Iso and Rf-Iso: ^{1}P3HT* + Ar-Iso → $P3HT^{+\bullet}$ + $Ar\text{-}Iso^{-\bullet}$, $-\Delta G_{CS}^{\circ} \sim 400$ mV; ^{1}P3HT* + Rf-Iso → $P3HT^{+\bullet}$ + $Rf\text{-}Iso^{-\bullet}$, $-\Delta G_{CS}^{\circ} \sim 430$ mV. If the role of the electron accepting material in an OPV includes augmenting the light harvesting capability of the donor polymer, factors other than the acceptor reduction potential and electronic absorptive properties need to be considered. In such an OPV, as electronically excited acceptors may be produced via direct light absorption or via an energy transfer reaction with an electronically excited donor polymer (e.g., ^{1}P3HT* + Ar-Iso → P3HT + ^{1}Ar-Iso*), engineering acceptor energy levels to facilitate exergonic photoinduced HT is critical. In this regard, it is important to appreciate that Ar-Iso and Rf-Iso possess significantly different driving forces for photoinduced HT reactions with P3HT: P3HT + ^{1}Ar-Iso* → $P3HT^{+\bullet}$ + $Ar\text{-}Iso^{-\bullet}$, $-\Delta G_{CS}^{\circ} \sim -20$ mV; P3HT + ^{1}Rf-Iso* → $P3HT^{+\bullet}$ + $Rf\text{-}Iso^{-\bullet}$, $-\Delta G_{CS}^{\circ} \sim 200$ mV. Thus, while both Ar-Iso and Rf-Iso may undergo phototoinduced ET reactions with electronically excited P3HT, only ^{1}Rf-Iso* is predicted to possess sufficient driving force to photo-oxidize ground-state P3HT, as these thermodynamic driving force considerations indicate that such a HT reaction involving ^{1}Ar-Iso* and P3HT would be endergonic.

Photovoltaic Devices Exhibiting Acceptor-Derived Photocurrent. OPV devices were produced for P3HT/Ar-Iso and P3HT/Rf-Iso in bilayer architectures; reference bulk heterojunction devices with P3HT/PCBM compositions were also studied. A conventional bilayer device configuration was employed consisting of ITO glass/PEDOT:PSS/P3HT/acceptor material/evaporated metal cathode; further fabrication details are available in the Supporting Information. As anticipated from the driving force considerations discussed above, no significant photocurrent [≥0.01% power conversion efficiency (PCE)] could be obtained from films of P3HT/Ar-

dx.doi.org/10.1021/ja5097418 | J. Am. Chem. Soc. 2014, 136, 17561−17569

Iso, while P3HT/Rf-Iso devices reliably gave efficiencies of 0.3−0.5%. These prototypical devices were not optimized, although several different film thicknesses were explored by variation of the revolution rate from 400 to 800 rpm in the Rf-Iso spin coating cycle. The best film, with an active layer of ∼90 nm thickness, gave PCEs that averaged at a modest 0.57%.

PCEs in P3HT solar cells that exploit molecular acceptors now approach 4%.[42] The best of these compositions, which featured a zinc(azadipyrromethene) complex as acceptor, exhibited a fill factor (FF) of 0.57, an open-circuit voltage (V_{OC}) of 0.76 V, and a short-circuit current (J_{SC}) of 8.8 mA/cm^2 (Table S1). The V_{OC} of 0.79 V determined for these P3HT/Rf-Iso devices is thus comparable to those reported for high-efficiency OPV compositions that feature molecular acceptors. In contrast, the best P3HT/Rf-Iso devices gave a J_{SC} of 2.43 mA·cm^{-2} and a fill factor of 0.29, values below the aforementioned benchmarks; these results suggest that suboptimal film morphologies played a role in the low efficiencies of Rf-Iso/P3HT devices by limiting the efficiency of charge carrier generation and collection.[2c] In this regard, it is noteworthy that Rf-Iso displayed negligible solubility in the absence of coordinating solvents; thus, these films were deposited from solutions of 2:8 THF/*o*-dichlorobenzene. Optimization of the deposition conditions for [(*meso*-perfluoroalkyl)porphinato]zinc(II)-based materials is likely to be a fruitful area of research but falls beyond the scope of the present work. A relationship between J_{SC} and $-\Delta G_{CS}$ has been established,[40c,e] and it is possible that the thermodynamic driving force of 200 mV for Rf-Iso/P3HT is insufficient to drive charge dissociation yields that approach unity in this system, which might also contribute to a low current density.

External quantum efficiency (EQE) spectra normalized to the peak efficiency of each composition for a P3HT/Rf-Iso film and a benchmark P3HT/PCBM OPV are depicted in Figure 4.

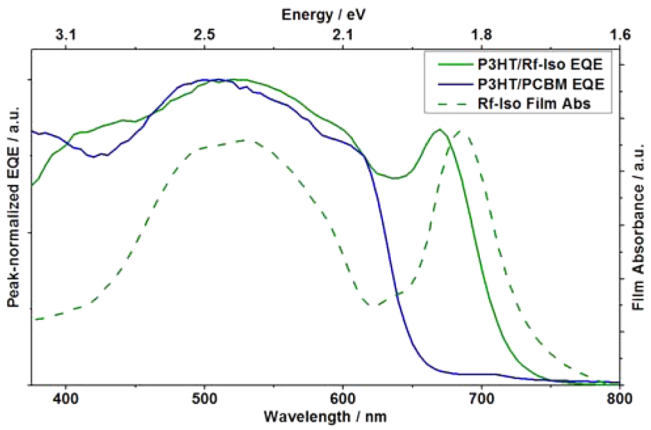

Figure 4. Peak-normalized EQE spectra from thin film OPV devices made from P3HT/Rf-Iso and P3HT/PCBM compositions, with the absorption spectrum of an Rf-Iso thin film for comparison.

In compositions with P3HT, PCBM is known to provide a negligible contribution to light harvesting at wavelengths beyond 375 nm; thus, the P3HT/PCBM spectrum provides a benchmark for P3HT-derived photocurrent.[43] The device using Rf-Iso as an acceptor shows an unmistakable contribution to its activity from the porphyrin derivative in the form of an EQE peak at 670 nm, with ∼15% of this film's integrated photocurrent produced beyond the long-wavelength onset for the P3HT/PCBM device at 650 nm. This NIR photocurrent is generated by photoinduced HT resulting from direct excitation of the Rf-Iso acceptor, sometimes called the channel-II path;[43] this observation highlights the importance of designing low band gap, strongly absorbing electron accepting materials that feature excited state reduction potentials ($E^{-/*}$ values) having sufficient driving force to undergo photoinduced HT with the ground-state donor polymer.

A prevalent first approximation for $-\Delta G_{CS}$ is the energetic offset between the frontier orbitals of D and A;[44] it is common practice to compare LUMO levels between D/A pairs to determine whether charge separation should be observable within a given system, with ∼0.3 eV typically assumed to be the threshold energetic offset below which electron transfer will not occur.[40e,45] Because the Ar-Iso and Rf-Iso LUMO levels are determined predominantly by the Iso unit, both Ar-Iso$^{-/0}$ and Rf-Iso$^{-/0}$ lie at ∼−3.6 eV versus vacuum; note that both of these values lie more than 0.3 eV below P3HT$^{-/0}$ (Figure 3). It has long been postulated that for systems in which the acceptor significantly contributes to light absorption, a similar comparison of D/A HOMO levels assesses the propensity for hole transfer from A to D;[44b] this finds that Rf-Iso$^{0/+}$ lies ∼0.4 eV below P3HT$^{0/+}$, while Ar-Iso$^{0/+}$ is 0.06 eV *above* this level. As the significance of channel-II photocurrent has become appreciated, the importance of molecular acceptor HOMO levels has recently garnered increased attention;[42f,g,43b,c] our findings underscore this significance by identifying at least one system (P3HT/Ar-Iso) where the lack of sufficient $-\Delta G_{CS}$ for hole transfer leads to PCEs of ∼ 0% at all wavelengths. Because the magnitudes of the Rf-Iso$^{0/+}$ and Ar-Iso$^{0/+}$ potentials are essentially determined by the nature of their respective PZn units, these data highlight the utility of the [5,15-(perfluoroalkyl)porphinato]zinc(II) building block, with an A$^{0/+}$ potential stabilized by ∼300 meV relative to common *meso*-arylporphyrin ligand frameworks, for the design of electron accepting chromophores for OPVs.

■ CONCLUSION

In summary, a supermolecular design strategy has afforded ethyne-conjugated isoindigo-(porphinato)zinc(II)-isoindigo chromophores built upon either electron-rich 10,20-diaryl-porphyrin (Ar-Iso) or electron-deficient 10,20-bis-(perfluoroalkyl)porphyrin (Rf-Iso) frameworks. Rf-Iso and Ar-Iso exhibit intense, porphyrin Q-state derived $S_0 \rightarrow S_1$ NIR transitions and total visible spectral domain integrated oscillator strengths that exceed 2; both Rf-Iso and Ar-Iso exhibit greater total absorptivities per unit mass than poly(3-hexyl)thiophene in the 375−900 nm wavelength range where solar flux is maximal. Time-dependent density functional theory calculations highlight the delocalized nature of the low energy singlet excited states of these chromophores and reveal that the extent of S_1 state charge-resonance character tracks with the extent of HOMO level destabilization. Prototype organic photovoltaic devices (OPVs) crafted from the donor poly(3-hexyl)thiophene and these new materials confirm that solar power conversion also depends critically upon the thermodynamic driving force for photoinduced hole transfer (HT) reactions involving these electronically excited low-band-gap acceptors and the ground-state poly(3-hexyl)thiophene (P3HT) polymer. While both the Rf-Iso and Ar-Iso supermolecules manifest LUMO levels poised for exergonic electron transfer (ET) from photoexcited P3HT (^{1}P3HT*), the [(perfluoroalkyl)porphinato]zinc unit of Rf-Iso engenders the electronically excited state of this chromophore

dx.doi.org/10.1021/ja5097418 | J. Am. Chem. Soc. 2014, 136, 17561−17569

(^{1}Rf-Iso*) with an excited state reduction potential ($E^{-/*}$) sufficient to drive hole transfer (HT) from ground-state P3HT.

This work highlights the effectiveness of coupled oscillator photophysics and the *meso*-perfluoroalkylporphyrin ligand framework for the design of an acceptor chromophore for OPVs that (i) possesses an excited-state reduction potential appropriate for photoinduced HT with the ground-state of the classic donor polymer P3HT, (ii) features a ground-state reduction potential appropriate for photoinduced ET with the electronically excited donor polymer (^{1}P3HT*), (iii) supersedes the total visible-range absorptivity of P3HT, and (iv) extends the device operating spectral range into the NIR. This work demonstrates for the first time that high oscillator strength porphyrinic chromophores, conventionally utilized as electron donors in OPVs, can also be exploited as electron acceptors.

■ ASSOCIATED CONTENT

Supporting Information

Synthetic details; characterization data; electrochemical data; TDDFT-computed frontier molecular orbitals, excited-state wave functions, spectra, and transition dipole moments; computational details; Ar-ETIPS and Rf-ETIPS absorption and emission spectra; photovoltaic device fabrication methods. This material is available free of charge via the Internet at http://pubs.acs.org.

■ AUTHOR INFORMATION

Corresponding Authors

wyou@unc.edu
michael.therien@duke.edu

Notes

The authors declare no competing financial interest.

■ ACKNOWLEDGMENTS

This material is based upon work wholly supported as part of the UNC EFRC: Center for Solar Fuels, an Energy Frontier Research Center funded by the U.S. Department of Energy, Office of Science, Office of Basic Energy Sciences under Award Number DE-SC0001011. The authors thank Nicholas Polizzi and Jaehong Park for many helpful discussions.

■ REFERENCES

(1) NREL; http://rredc.nrel.gov/solar/spectra/am1.5/; accessed Dec 9th, 2013.

(2) (a) Schlenker, C. W.; Thompson, M. E. *Top. Curr. Chem.* **2012**, *312*, 175−212. (b) Kirchartz, T.; Agostinelli, T.; Campoy-Quiles, M.; Gong, W.; Nelson, J. *J. Phys. Chem. Lett.* **2012**, *3*, 3470−3475. (c) Heeger, A. J. *Adv. Mater.* **2013**, *26*, 10−28.

(3) (a) Ferguson, A. J.; Kopidakis, N.; Shaheen, S. E.; Rumbles, G. *J. Phys. Chem. C* **2011**, *115*, 23134−23148. (b) Liu, T.; Cheung, D. L.; Troisi, A. *Phys. Chem. Chem. Phys.* **2011**, *13*, 21461−21470. (c) Jin, H.; Pivrikas, A.; Lee, K. H.; Aljada, M.; Hambsch, M.; Burn, P. L.; Meredith, P. *Adv. Energy Mater.* **2012**, *2*, 1338−1342.

(4) (a) Chen, H.-Y.; Hou, J.; Zhang, S.; Liang, Y.; Yang, G.; Yang, Y.; Yu, L.; Wu, Y.; Li, G. *Nat. Photonics* **2009**, *3*, 649−653. (b) Su, M.-S.; Kuo, C.-Y.; Yuan, M.-C.; Jeng, U.-S.; Su, C.-J.; Wei, K.-H. *Adv. Mater.* **2011**, *23*, 3315−3319. (c) Zhou, H.; Yang, L.; Stuart, A. C.; Price, S. C.; Liu, S.; You, W. *Angew. Chem., Int. Ed.* **2011**, *50*, 2995−2998. (d) He, Z.; Zhong, C.; Su, S.; Xu, M.; Wu, H.; Cao, Y. *Nat. Photonics* **2012**, *6*, 591−595. (e) Small, C. E.; Chen, S.; Subbiah, J.; Amb, C. M.; Tsang, S.-W.; Lai, T.-H.; Reynolds, J. R.; So, F. *Nat. Photonics* **2012**, *6*, 115−120. (f) Tan, Z. a.; Zhang, W.; Zhang, Z.; Qian, D.; Huang, Y.; Hou, J.; Li, Y. *Adv. Mater.* **2012**, *24*, 1476−1481. (g) You, J.; Chen, C.-C.; Dou, L.; Murase, S.; Duan, H.-S.; Hawks, S. A.; Xu, T.; Son, H. J.; Yu, L.; Li, G.; Yang, Y. *Adv. Mater.* **2012**, *24*, 5267−5272.

(5) You, J.; Dou, L.; Yoshimura, K.; Kato, T.; Ohya, K.; Moriarty, T.; Emery, K.; Chen, C.-C.; Gao, J.; Li, G.; Yang, Y. *Nat. Commun.* **2013**, *4*, 1446.

(6) (a) Steinmann, V.; Kronenberg, N. M.; Lenze, M. R.; Graf, S. M.; Hertel, D.; Meerholz, K.; Bürckstümmer, H.; Tulyakova, E. V.; Würthner, F. *Adv. Energy Mater.* **2011**, *1*, 888−893. (b) Wei, G.; Wang, S.; Sun, K.; Thompson, M. E.; Forrest, S. R. *Adv. Energy Mater.* **2011**, *1*, 184−187. (c) Zhou, J.; Wan, X.; Liu, Y.; Long, G.; Wang, F.; Li, Z.; Zuo, Y.; Li, C.; Chen, Y. *Chem. Mater.* **2011**, *23*, 4666−4668. (d) Chiu, S.-W.; Lin, L.-Y.; Lin, H.-W.; Chen, Y.-H.; Huang, Z.-Y.; Lin, Y.-T.; Lin, F.; Liu, Y.-H.; Wong, K.-T. *Chem. Commun.* **2012**, *48*, 1857−1859. (e) Sun, Y.; Welch, G. C.; Leong, W. L.; Takacs, C. J.; Bazan, G. C.; Heeger, A. J. *Nat. Mater.* **2012**, *11*, 44−48. (f) Bura, T.; Leclerc, N.; Fall, S.; Leveque, P.; Heiser, T.; Retailleau, P.; Rihn, S.; Mirloup, A.; Ziessel, R. *J. Am. Chem. Soc.* **2012**, *134*, 17404−17407. (g) Bura, T.; Leclerc, N.; Bechara, R.; Leveque, P.; Heiser, T.; Ziessel, R. *Adv. Energy Mater.* **2013**, *3*, 1118−1124. (h) Kyaw, A. K. K.; Wang, D. H.; Wynands, D.; Zhang, J.; Nguyen, T.-Q.; Bazan, G. C.; Heeger, A. J. *Nano Lett.* **2013**, *13*, 3796−3801.

(7) (a) Green, M. A.; Emery, K.; Hishikawa, Y.; Warta, W.; Dunlop, E. D. *Prog. Photovoltaics Res. Appl.* **2014**, *22*, 701−710. (b) Carlé, J. E.; Krebs, F. C. *Sol. Energy Mater. Sol. Cells* **2013**, *119*, 309−310.

(8) An, Z.; Odom, S. A.; Kelley, R. F.; Huang, C.; Zhang, X.; Barlow, S.; Padilha, L. A.; Fu, J.; Webster, S.; Hagan, D. J.; Van Stryland, E. W.; Wasielewski, M. R.; Marder, S. R. *J. Phys. Chem. A* **2009**, *113*, 5585−5593.

(9) Rodríguez-Morgade, M. S.; Claessens, C. G.; Medina, A.; González-Rodríguez, D.; Gutiérrez-Puebla, E.; Monge, A.; Alkorta, I.; Elguero, J.; Torres, T. *Chem.—Eur. J.* **2008**, *14*, 1342−1350.

(10) (a) DiMagno, S. G.; Williams, R. A.; Therien, M. J. *J. Org. Chem.* **1994**, *59*, 6943−6948. (b) Goll, J. G.; Moore, K. T.; Ghosh, A.; Therien, M. J. *J. Am. Chem. Soc.* **1996**, *118*, 8344−8354. (c) Wertsching, A. K.; Koch, A. S.; DiMagno, S. G. *J. Am. Chem. Soc.* **2001**, *123*, 3932−3939.

(11) (a) Ahmed, E.; Ren, G.; Kim, F. S.; Hollenbeck, E. C.; Jenekhe, S. A. *Chem. Mater.* **2011**, *23*, 4563−4577. (b) Huang, C.; Barlow, S.; Marder, S. R. *J. Org. Chem.* **2011**, *76*, 2386−2407. (c) Mei, J.; Graham, K. R.; Stalder, R.; Reynolds, J. R. *Org. Lett.* **2010**, *12*, 660−663.

(12) (a) Zhao, Y.; Wasielewski, M. R. *Tetrahedron Lett.* **1999**, *40*, 7047−7050. (b) Serin, J. M.; Brousmiche, D. W.; Fréchet, J. M. J. *J. Am. Chem. Soc.* **2002**, *124*, 11848−11849.

(13) (a) Lin, V. S.-Y.; DiMagno, S. G.; Therien, M. J. *Science* **1994**, *264*, 1105−1111. (b) Lin, V. S.-Y.; Therien, M. J. *Chem.—Eur. J.* **1995**, *1*, 645−651. (c) Kumble, R.; Palese, S.; Lin, V. S.-Y.; Therien, M. J.; Hochstrasser, R. M. *J. Am. Chem. Soc.* **1998**, *120*, 11489−11498. (d) Shediac, R.; Gray, M. H. B.; Uyeda, H. T.; Johnson, R. C.; Hupp, J. T.; Angiolillo, P. J.; Therien, M. J. *J. Am. Chem. Soc.* **2000**, *122*, 7017−7033. (e) Angiolillo, P. J.; Susumu, K.; Uyeda, H. T.; Lin, V. S.-Y.; Shediac, R.; Therien, M. J. *Synth. Met.* **2001**, *116*, 247−253. (f) Susumu, K.; Therien, M. J. *J. Am. Chem. Soc.* **2002**, *124*, 8550−8552. (g) Rubtsov, I. V.; Susumu, K.; Rubtsov, G. I.; Therien, M. J. *J. Am. Chem. Soc.* **2003**, *125*, 2687−2696. (h) Angiolillo, P. J.; Uyeda, H. T.; Duncan, T. V.; Therien, M. J. *J. Phys. Chem. B* **2004**, *108*, 11893−11903. (i) Susumu, K.; Duncan, T. V.; Therien, M. J. *J. Am. Chem. Soc.* **2005**, *127*, 5186−5195. (j) Duncan, T. V.; Susumu, K.; Sinks, L. E.; Therien, M. J. *J. Am. Chem. Soc.* **2006**, *128*, 9000−9001. (k) Duncan, T. V.; Wu, S. P.; Therien, M. J. *J. Am. Chem. Soc.* **2006**, *128*, 10423−10435. (l) Susumu, K.; Frail, P. R.; Angiolillo, P. J.; Therien, M. J. *J. Am. Chem. Soc.* **2006**, *128*, 8380−8381. (m) Strzalka, J.; Xu, T.; Tronin, A.; Wu, S. P.; Miloradovic, I.; Kuzmenko, I.; Gog, T.; Therien, M. J.; Blasie, J. K. *Nano Lett.* **2006**, *6*, 2395−2405. (n) Frail, P. R.; Susumu, K.; Huynh, M.; Fong, J.; Kikkawa, J. M.; Therien, M. J. *Chem. Mater.* **2007**, *19*, 6062−6064. (o) Duncan, T. V.; Frail, P. R.; Miloradovic, I. R.; Therien, M. J. *J. Phys. Chem. B* **2010**, *114*, 14696−14702. (p) Li, Z.; Park, T.-H.; Rawson, J.; Therien, M. J.; Borguet, E. *Nano Lett.* **2012**, *12*, 2722−2727.

(14) (a) Uyeda, H. T.; Zhao, Y.; Wostyn, K.; Asselberghs, I.; Clays, K.; Persoons, A.; Therien, M. J. *J. Am. Chem. Soc.* **2002**, *124*, 13806−13813. (b) Duncan, T. V.; Rubtsov, I. V.; Uyeda, H. T.; Therien, M. J. *J. Am. Chem. Soc.* **2004**, *126*, 9474−9475. (c) Duncan, T. V.; Ishizuka, T.; Therien, M. J. *J. Am. Chem. Soc.* **2007**, *129*, 9691−9703. (d) Duncan, T. V.; Song, K.; Hung, S.-T.; Miloradovic, I.; Nayak, A.; Persoons, A.; Verbiest, T.; Therien, M. J.; Clays, K. *Angew. Chem., Int. Ed.* **2008**, *47*, 2978−2981. (e) Keinan, S.; Therien, M. J.; Beratan, D. N.; Yang, W. *J. Phys. Chem. A* **2008**, *112*, 12203−12207. (f) Hu, X.; Xiao, D.; Keinan, S.; Asselberghs, I.; Therien, M. J.; Clays, K.; Yang, W.; Beratan, D. N. *J. Phys. Chem. C* **2010**, *114*, 2349−2359. (g) Singh-Rachford, T. N.; Nayak, A.; Muro-Small, M. L.; Goeb, S.; Therien, M. J.; Castellano, F. N. *J. Am. Chem. Soc.* **2010**, *132*, 14203−14211.

(15) (a) Kim, D. *Multiporphyrin Arrays: Fundamentals and Applications*; Pan Stanford: Singapore, 2012. (b) Panda, M. K.; Ladomenou, K.; Coutsolelos, A. G. *Coord. Chem. Rev.* **2012**, *256*, 2601−2627.

(16) (a) LeCours, S. M.; DiMagno, S. G.; Therien, M. J. *J. Am. Chem. Soc.* **1996**, *118*, 11854−11864. (b) LeCours, S. M.; Guan, H.-W.; DiMagno, S. G.; Wang, C. H.; Therien, M. J. *J. Am. Chem. Soc.* **1996**, *118*, 1497−1503. (c) Angiolillo, P. J.; Rawson, J.; Frail, P. R.; Therien, M. J. *Chem. Commun.* **2013**, *49*, 9722−9724.

(17) (a) Anderson, H. L.; Wylie, A. P.; Prout, K. *J. Chem. Soc., Perkin Trans. 1* **1998**, 1607−1612. (b) Taylor, P. N.; Wylie, A. P.; Huuskonen, J.; Anderson, H. L. *Angew. Chem., Int. Ed.* **1998**, *37*, 986−989. (c) Yen, W.-N.; Lo, S.-S.; Kuo, M.-C.; Mai, C.-L.; Lee, G.-H.; Peng, S.-M.; Yeh, C.-Y. *Org. Lett.* **2006**, *8*, 4239−4242. (d) Kuo, M.-C.; Li, L.-A.; Yen, W.-N.; Lo, S.-S.; Lee, C.-W.; Yeh, C.-Y. *Dalton Trans.* **2007**, 1433−1439. (e) Odom, S. A.; Kelley, R. F.; Ohira, S.; Ensley, T. R.; Huang, C.; Padilha, L. A.; Webster, S.; Coropceanu, V.; Barlow, S.; Hagan, D. J.; Van Stryland, E. W.; Brédas, J.-L.; Anderson, H. L.; Wasielewski, M. R.; Marder, S. R. *J. Phys. Chem. A* **2009**, *113*, 10826−10832. (f) Odom, S. A.; Webster, S.; Padilha, L. A.; Peceli, D.; Hu, H.; Nootz, G.; Chung, S.-J.; Ohira, S.; Matichak, J. D.; Przhonska, O. V.; Kachkovski, A. D.; Barlow, S.; Brédas, J.-L.; Anderson, H. L.; Hagan, D. J.; Van Stryland, E. W.; Marder, S. R. *J. Am. Chem. Soc.* **2009**, *131*, 7510−7511. (g) Nowak-Król, A.; Koszarna, B.; Yoo, S. Y.; Chromiński, J.; Węcławski, M. K.; Lee, C.-H.; Gryko, D. T. *J. Org. Chem.* **2011**, *76*, 2627−2634. (h) Nowak-Król, A.; Wilson, C. J.; Drobizhev, M.; Kondratuk, D. V.; Rebane, A.; Anderson, H. L.; Gryko, D. T. *ChemPhysChem* **2012**, *13*, 3966−3972.

(18) (a) Cho, E. H.; Chae, S. H.; Kim, K.; Lee, S. J.; Joo, J. *Synth. Met.* **2012**, *162*, 813−819. (b) Hatano, J.; Obata, N.; Yamaguchi, S.; Yasuda, T.; Matsuo, Y. *J. Mater. Chem.* **2012**, *22*, 19258−19263. (c) Huang, Y.; Li, L.; Peng, X.; Peng, J.; Cao, Y. *J. Mater. Chem.* **2012**, *22*, 21841−21844. (d) Li, L.; Huang, Y.; Peng, J.; Cao, Y.; Peng, X. *J. Mater. Chem. A* **2013**, *1*, 2144−2150. (e) Yamamoto, T.; Hatano, J.; Nakagawa, T.; Yamaguchi, S.; Matsuo, Y. *Appl. Phys. Lett.* **2013**, *102*, 013305.

(19) (a) Bessho, T.; Zakeeruddin, S. M.; Yeh, C.-Y.; Diau, E. W.-G.; Grätzel, M. *Angew. Chem., Int. Ed.* **2010**, *49*, 6646−6649. (b) Mai, C.-L.; Huang, W.-K.; Lu, H.-P.; Lee, C.-W.; Chiu, C.-L.; Liang, Y.-R.; Diau, E. W.-G.; Yeh, C.-Y. *Chem. Commun.* **2010**, *46*, 809−811. (c) Liu, Y.; Lin, H.; Dy, J. T.; Tamaki, K.; Nakazaki, J.; Nakayama, D.; Uchida, S.; Kubo, T.; Segawa, H. *Chem. Commun.* **2011**, *47*, 4010−4012. (d) Li, L.-L.; Diau, E. W.-G. *Chem. Soc. Rev.* **2013**, *42*, 291−304. (e) Hamamura, T.; Dy, J. T.; Tamaki, K.; Nakazaki, J.; Uchida, S.; Kubo, T.; Segawa, H. *Phys. Chem. Chem. Phys.* **2014**, *16*, 4551−4560.

(20) (a) Luechai, A.; Gasiorowski, J.; Petsom, A.; Neugebauer, H.; Sariciftci, N. S.; Thamyongkit, P. *J. Mater. Chem.* **2012**, *22*, 23030−23037. (b) Kengthanomma, T.; Thamyongkit, P.; Gasiorowski, J.; Ramil, A. M.; Sariciftci, N. S. *J. Mater. Chem. A* **2013**, *1*, 10524−10531.

(21) (a) Moore, K. T.; Horváth, I. T.; Therien, M. J. *J. Am. Chem. Soc.* **1997**, *119*, 1791−1792. (b) Woller, E. K.; DiMagno, S. G. *J. Org. Chem.* **1997**, *62*, 1588−1593. (c) Moore, K. T.; Fletcher, J. T.; Therien, M. J. *J. Am. Chem. Soc.* **1999**, *121*, 5196−5209.

(22) (a) Stalder, R.; Mei, J.; Graham, K. R.; Estrada, L. A.; Reynolds, J. R. *Chem. Mater.* **2014**, *26*, 664−678. (b) Lei, T.; Wang, J.-Y.; Pei, J. *Acc. Chem. Res.* **2014**, *47*, 1117−1126. (c) Wang, E.; Mammo, W.; Andersson, M. R. *Adv. Mater.* **2014**, *26*, 1801−1826.

(23) (a) Ashraf, R. S.; Kronemeijer, A. J.; James, D. I.; Sirringhaus, H.; McCulloch, I. *Chem. Commun.* **2012**, *48*, 3939−3941. (b) Lei, T.; Dou, J.-H.; Ma, Z.-J.; Yao, C.-H.; Liu, C.-J.; Wang, J.-Y.; Pei, J. *J. Am. Chem. Soc.* **2012**, *134*, 20025−20028. (c) Grenier, F.; Berrouard, P.; Pouliot, J.-R.; Tseng, H.-R.; Heeger, A. J.; Leclerc, M. *Polym. Chem.* **2013**, *4*, 1836−1841. (d) Lei, T.; Dou, J.-H.; Ma, Z.-J.; Liu, C.-J.; Wang, J.-Y.; Pei, J. *Chem. Sci.* **2013**, *4*, 2447−2452.

(24) (a) Liu, B.; Zou, Y.; Peng, B.; Zhao, B.; Huang, K.; He, Y.; Pan, C. *Polym. Chem.* **2011**, *2*, 1156−1162. (b) Ma, Z.-F.; Wang, E.-g.; K; Andersson, M. R.; Zhang, F.-L. *Appl. Phys. Lett.* **2011**, *99*, 143302. (c) Zhang, G.; Fu, Y.; Xie, Z.; Zhang, Q. *Macromolecules* **2011**, *44*, 1414−1420. (d) Wang, E.; Ma, Z.; Zhang, Z.; K; Henriksson, P.; Inganas, O.; Zhang, F.; Andersson, M. R. *J. Am. Chem. Soc.* **2011**, *133*, 14244−14247. (e) Wang, E.; Ma, Z.; Zhang, Z.; Henriksson, P.; Inganaes, O.; Zhang, F.; Andersson, M. R. *Chem. Commun.* **2011**, *47*, 4908−4910. (f) Ma, Z.; Wang, E.; Jarvid, M. E.; Henriksson, P.; Inganaes, O.; Zhang, F.; Andersson, M. R. *J. Mater. Chem.* **2012**, *22*, 2306−2314. (g) Hu, C.; Fu, Y.; Li, S.; Xie, Z.; Zhang, Q. *Polym. Chem.* **2012**, *3*, 2949−2955. (h) Stalder, R.; Grand, C.; Subbiah, J.; So, F.; Reynolds, J. R. *Polym. Chem.* **2012**, *3*, 89−92. (i) K; Ma, Z.; Bergqvist, J.; Tang, Z.; Wang, E.; Henriksson, P.; Tvingstedt, K.; Andersson, M. R.; Zhang, F.; Inganaes, O. *Adv. Funct. Mater.* **2012**, *22*, 3480−3490. (j) Cao, K.; Wu, Z.; Li, S.; Sun, B.; Zhang, G.; Zhang, Q. *J. Polym. Sci., Part A: Polym. Chem.* **2013**, *51*, 94−100. (k) Chen, M. S.; Niskala, J. R.; Unruh, D. A.; Chu, C. K.; Lee, O. P.; Fréchet, J. M. J. *Chem. Mater.* **2013**, *25*, 4088−4096. (l) Dang, D.; Chen, W.; Yang, R.; Zhu, W.; Mammo, W.; Wang, E. *Chem. Commun.* **2013**, *49*, 9335−9337. (m) Ho, C.-C.; Chang, S.-Y.; Huang, T.-C.; Chen, C.-A.; Liao, H.-C.; Chen, Y.-F.; Su, W.-F. *Polym. Chem.* **2013**, *4*, 5351−5360. (n) Mahmood, K.; Liu, Z.-P.; Li, C.; Lu, Z.; Fang, T.; Liu, X.; Zhou, J.; Lei, T.; Pei, J.; Bo, Z. *Polym. Chem.* **2013**, *4*, 3563−3574. (o) Sonar, P.; Tan, H.-S.; Sun, S.; Lam, Y. M.; Dodabalapur, A. *Polym. Chem.* **2013**, *4*, 1983−1994. (p) Wan, M.; Zhu, H.; Deng, H.; Jin, L.; Guo, J.; Huang, Y. *J. Polym. Sci., Part A: Polym. Chem.* **2013**, *51*, 3477−3485. (q) Wang, C.; Zhao, B.; Cao, Z.; Shen, P.; Tan, Z.; Li, X.; Tan, S. *Chem. Commun.* **2013**, *49*, 3857−3859. (r) Xu, X.; Cai, P.; Lu, Y.; Choon, N. S.; Chen, J.; Hu, X.; Ong, B. S. *J. Polym. Sci., Part A: Polym. Chem.* **2013**, *51*, 424−434.

(25) (a) Graham, K. R.; Mei, J.; Stalder, R.; Shim, J. W.; Cheun, H.; Steffy, F.; So, F.; Kippelen, B.; Reynolds, J. R. *ACS Appl. Mater. Interfaces* **2011**, *3*, 1210−1215. (b) Graham, K. R.; Wieruszewski, P. M.; Stalder, R.; Hartel, M. J.; Mei, J.; So, F.; Reynolds, J. R. *Adv. Funct. Mater.* **2012**, *22*, 4801−4813. (c) Elsawy, W.; Lee, C.-L.; Cho, S.; Oh, S.-H.; Moon, S.-H.; Elbarbary, A.; Lee, J.-S. *Phys. Chem. Chem. Phys.* **2013**, *15*, 15193−15203. (d) Karakawa, M.; Aso, Y. *RSC Adv.* **2013**, *3*, 16259−16263. (e) Liu, Q.; Du, Z.; Chen, W.; Sun, L.; Chen, Y.; Sun, M.; Yang, R. *Synth. Met.* **2013**, *178*, 38−43. (f) Wang, T.; Chen, Y.; Bao, X.; Du, Z.; Guo, J.; Wang, N.; Sun, M.; Yang, R. *Dyes Pigm.* **2013**, *98*, 11−16. (g) Yang, M.; Chen, X.; Zou, Y.; Pan, C.; Liu, B.; Zhong, H. *J. Mater. Sci.* **2013**, *48*, 1014−1020. (h) Yassin, A.; Leriche, P.; Allain, M.; Roncali, J. *New J. Chem.* **2013**, *37*, 502−507.

(26) Stalder, R.; Mei, J.-G.; Subbiah, J.; Grand, C.; Estrada, L. A.; So, F.; Reynolds, J. R. *Macromolecules* **2011**, *44*, 6303−6310.

(27) Lunak, S., Jr.; Horakova, P.; Lycka, A. *Dyes Pigm.* **2010**, *85*, 171−176.

(28) Frisch, M. J.; Trucks, G. W.; Schlegel, H. B.; Scuseria, G. E.; Robb, M. A.; Cheeseman, J. R.; Scalmani, G.; Barone, V.; Mennucci, B.; Petersson, G. A.; Nakatsuji, H.; Caricato, M.; Li, X.; Hratchian, H. P.; Izmaylov, A. F.; Bloino, J.; Zheng, G.; Sonnenberg, J. L.; Hada, M.; Ehara, M.; Toyota, K.; Fukuda, R.; Hasegawa, J.; Ishida, M.; Nakajima, T.; Honda, Y.; Kitao, O.; Nakai, H.; Vreven, T.; Montgomery, J. A., Jr.; Peralta, J. E.; Ogliaro, F.; Bearpark, M.; Heyd, J. J.; Brothers, E.; Kudin, K. N.; Staroverov, V. N.; Kobayashi, R.; Normand, J.; Raghavachari, K.; Rendell, A.; Burant, J. C.; Iyengar, S. S.; Tomasi, J.; Cossi, M.; Rega, N.; Millam, J. M.; Klene, M.; Knox, J. E.; Cross, J. B.; Bakken, V.; Adamo, C.; Jaramillo, J.; Gomperts, R.; Stratmann, R. E.; Yazyev, O.; Austin, A. J.; Cammi, R.; Pomelli, C.; Ochterski, J. W.; Martin, R. L.;

Morokuma, K.; Zakrzewski, V. G.; Voth, G. A.; Salvador, P.; Dannenberg, J. J.; Dapprich, S.; Daniels, A. D.; Farkas, O.; Foresman, J. B.; Ortiz, J. V.; Cioslowski, J.; Fox, D. J. *Gaussian 09*, revision C.1; Gaussian, Inc.: Wallingford, CT, 2009.
(29) Becke, A. D. *J. Chem. Phys.* **1993**, *98*, 5648−5652.
(30) (a) Lee, C.; Yang, W.; Parr, R. G. *Phys. Rev. B* **1988**, *37*, 785−789. (b) Miehlich, B.; Savin, A.; Stoll, H.; Preuss, H. *Chem. Phys. Lett.* **1989**, *157*, 200−206.
(31) (a) Binning, R. C.; Curtiss, L. A. *J. Comput. Chem.* **1990**, *11*, 1206−1216. (b) Blaudeau, J.-P.; McGrath, M. P.; Curtiss, L. A.; Radom, L. *J. Chem. Phys.* **1997**, *107*, 5016−5021. (c) Curtiss, L. A.; McGrath, M. P.; Blaudeau, J.-P.; Davis, N. E.; Binning, J. R. C.; Radom, L. *J. Chem. Phys.* **1995**, *103*, 6104−6113. (d) Hay, P. J. *J. Chem. Phys.* **1977**, *66*, 4377−4384. (e) Krishnan, R.; Binkley, J. S.; Seeger, R.; Pople, J. A. *J. Chem. Phys.* **1980**, *72*, 650−654. (f) McGrath, M. P.; Radom, L. *J. Chem. Phys.* **1991**, *94*, 511−516. (g) McLean, A. D.; Chandler, G. S. *J. Chem. Phys.* **1980**, *72*, 5639−5648. (h) Raghavachari, K.; Trucks, G. W. *J. Chem. Phys.* **1989**, *91*, 1062−1065. (i) Wachters, A. J. H. *J. Chem. Phys.* **1970**, *52*, 1033−1036.
(32) Dennington, R.; Keith, T.; Millam, J. *GaussView*, version 5; Semichem Inc.: Shawnee Mission, KS, 2009.
(33) O'Boyle, N. M.; Tenderholt, A. L.; Langner, K. M. *J. Comput. Chem.* **2008**, *29*, 839−845.
(34) Mulliken, R. S. *J. Chem. Phys.* **1955**, *23*, 1833−1840.
(35) Humphrey, W.; Dalke, A.; Schulten, K. *J. Mol. Graphics* **1996**, *14*, 33−38.
(36) Wienk, M. M.; Kroon, J. M.; Verhees, W. J. H.; Knol, J.; Hummelen, J. C.; van Hal, P. A.; Janssen, R. A. J. *Angew. Chem., Int. Ed.* **2003**, *42*, 3371−3375.
(37) Xu, T.; Wu, S. P.; Miloradovic, I.; Therien, M. J.; Blasie, J. K. *Nano Lett.* **2006**, *6*, 2387−2394.
(38) Gouterman, M. *J. Mol. Spectrosc.* **1961**, *6*, 138−163.
(39) Takacs, C. J.; Sun, Y.; Welch, G. C.; Perez, L. A.; Liu, X.; Wen, W.; Bazan, G. C.; Heeger, A. J. *J. Am. Chem. Soc.* **2012**, *134*, 16597−16606.
(40) (a) Weller, A. *Z. Phys. Chem.* **1982**, *133*, 93−98. (b) Juris, A.; Balzani, V.; Barigelletti, F.; Campagna, S.; Belser, P.; von Zelewsky, A. *Coord. Chem. Rev.* **1988**, *84*, 85−277. (c) Rand, B. P.; Burk, D. P.; Forrest, S. R. *Phys. Rev. B* **2007**, *75*, 115327. (d) Veldman, D.; Meskers, S. C. J.; Janssen, R. A. J. *Adv. Funct. Mater.* **2009**, *19*, 1939−1948. (e) Dimitrov, S. D.; Durrant, J. R. *Chem. Mater.* **2014**, *26*, 616−630.
(41) Several competing values for the Fc/Fc^+ work function are prevalent in the literature. By selecting one and applying it uniformly to our own potentiometric data referenced to an internal standard, we hope to minimize ambiguity. For more, see Cardona, C. M.; Li, W.; Kaifer, A. E.; Stockdale, D.; Bazan, G. C. *Adv. Mater.* **2011**, *23*, 2367−2371.
(42) (a) Bloking, J. T.; Han, X.; Higgs, A. T.; Kastrop, J. P.; Pandey, L.; Norton, J. E.; Risko, C.; Chen, C. E.; Brédas, J.-L.; McGehee, M. D.; Sellinger, A. *Chem. Mater.* **2011**, *23*, 5484−5490. (b) Zhou, Y.; Dai, Y.-Z.; Zheng, Y.-Q.; Wang, X.-Y.; Wang, J.-Y.; Pei, J. *Chem. Commun.* **2013**, *49*, 5802−5804. (c) Winzenberg, K. N.; Kemppinen, P.; Scholes, F. H.; Collis, G. E.; Shu, Y.; Birendra Singh, T.; Bilic, A.; Forsyth, C. M.; Watkins, S. E. *Chem. Commun.* **2013**, *49*, 6307−6309. (d) Yan, Q.; Zhou, Y.; Zheng, Y.-Q.; Pei, J.; Zhao, D. *Chem. Sci.* **2013**, *4*, 4389−4394. (e) Kim, H. U.; Kim, J.-H.; Suh, H.; Kwak, J.; Kim, D.; Grimsdale, A. C.; Yoon, S. C.; Hwang, D.-H. *Chem. Commun.* **2013**, *49*, 10950−10952. (f) Douglas, J. D.; Chen, M. S.; Niskala, J. R.; Lee, O. P.; Yiu, A. T.; Young, E. P.; Fréchet, J. M. J. *Adv. Mater.* **2014**, *26*, 4606−4606. (g) Mao, Z.; Senevirathna, W.; Liao, J.-Y.; Gu, J.; Kesava, S. V.; Guo, C.; Gomez, E. D.; Sauvé, G. *Adv. Mater.* **2014**, *26*, 6290−6294.
(43) (a) Zhang, Y.; Pandey, A. K.; Tandy, K.; Dutta, G. K.; Burn, P. L.; Meredith, P.; Namdas, E. B.; Patil, S. *Appl. Phys. Lett.* **2013**, *102*, 223302. (b) Fang, Y.; Pandey, A. K.; Nardes, A. M.; Kopidakis, N.; Burn, P. L.; Meredith, P. *Adv. Energy Mater.* **2013**, *3*, 54−59. (c) Pho, T. V.; Toma, F. M.; Tremolet de Villers, B. J.; Wang, S.; Treat, N. D.; Eisenmenger, N. D.; Su, G. M.; Coffin, R. C.; Douglas, J. D.; Fréchet, J. M. J.; Bazan, G. C.; Wudl, F.; Chabinyc, M. L. *Adv. Energy Mater.* **2014**, *4*, 1301007.
(44) (a) Brabec, C. J.; Winder, C.; Sariciftci, N. S.; Hummelen, J. C.; Dhanabalan, A.; van Hal, P. A.; Janssen, R. A. J. *Adv. Funct. Mater.* **2002**, *12*, 709−712. (b) Brédas, J.-L.; Beljonne, D.; Coropceanu, V.; Cornil, J. *Chem. Rev.* **2004**, *104*, 4971−5004.
(45) (a) Scharber, M. C.; Mühlbacher, D.; Koppe, M.; Denk, P.; Waldauf, C.; Heeger, A. J.; Brabec, C. J. *Adv. Mater.* **2006**, *18*, 789−794. (b) Su, Y.-W.; Lan, S.-C.; Wei, K.-H. *Mater. Today* **2012**, *15*, 554−562.